Structural effects of hydrostatic pressure in $Sr_{1-x}M_xCuO_2$ (M = La,Ca) and $Sr_4Cu_6O_{10}$

H. Shaked,* Y. Shimakawa,† B. A. Hunter, P. G. Radaelli, B. Dabrowski, R. L. Hitterman, and J. D. Jorgensen
Materials Science Division, Argonne National Laboratory, Argonne, Illinois 60439

P. D. Han and D. A. Payne
Materials Science and Engineering Department, University of Illinois, Urbana, Illinois 61801

S. Kikkawa, G. Er, and F. Kanamaru
The Institute of Scientific and Industrial Research, Osaka University, 8-1 Mihogaoka, Ibaraki, Osaka 567, Japan
(Received 23 June 1994)

Pressure effects on the tetragonal infinite-layer structure were studied in superconducting $Sr_{0.9}La_{0.1}CuO_2$ (electron-doped) and $Sr_{0.7}Ca_{0.3}CuO_2$ (hole-doped) samples, and in an insulating nonsuperconducting $Sr_{0.14}Ca_{0.86}CuO_2$ sample, using time-of-flight neutron powder diffraction. Neutron-diffraction measurements, with the sample at room temperature, were performed at several hydrostatic pressures up to ≈ 0.6 GPa on each of the three samples, using a helium-gas pressure cell. The measured compressibilities, which are similar for the three samples, show a large anisotropy, and are in a good agreement with first-principles calculations performed for undoped $Sr_{0.7}Ca_{0.3}CuO_2$. Atomic size effects of the A atom in $ACuO_2$ on the crystal lattice are discussed and are compared with the pressure effects. A relation is found between the in-plane compressibilities among n-layer ($n = 1,2,3\ldots,\infty$) structures of high-T_c superconductors.

I. INTRODUCTION

The effect of pressure on T_c and its relation to pressure-induced crystallographic changes in high-T_c superconductors (HTSC's) have been the subject of numerous studies.[1] It is believed that one way pressure affects T_c is via its effect on carrier concentration. There are, however, in addition, intrinsic structural contributions to the pressure effect on T_c, which arise from the effect of pressure on the Cu-O bond length (interplane) and intraplane separation at a constant carrier concentration.[1,2] In hole-doped HTSC it is generally found that the pressure derivative of T_c, dT_c/dP, is positive.[1] The remarkable pressure-induced increase in T_c in $HgBa_2Ca_2Cu_3O_8$ (Hg-1223) from 134 K (ambient) to 153 K (15 GPa),[3] and to 164 K (30 GPa) (Ref. 4) generated renewed interest in pressure effects on HTCS's. These papers were immediately followed by a study[5] of pressure-induced crystallographic changes in Hg-1201, Hg-1212, and Hg-1223. In this study, compressibilities of four bond lengths, two within and two between the conducting blocks of CuO_2 layers are reported. The difficult question of the relation between these four bond compressibilities and the pressure derivative of T_c was addressed in this paper. It is intuitively clear that as the number of CuO_2 planes per conducting block n increases, the effect of the bonds external to the conducting block on dT_C/dP should decrease. At the extreme, when n is very large, one obtains the simplest structure among all HTSC's, the infinite-layer (IL) structure (Fig. 1).[6] This structure has only two bond lengths, and the problem of relating bond length changes to changes in T_c is considerably simplified.

The first cuprate synthesized in the infinite layer (IL) structure was $Sr_{0.14}Ca_{0.86}CuO_2$,[6] which was found to be antiferromagnetic and not superconducting. It was possible to stabilize the IL structure at ambient oxygen pressure only in a narrow range near this composition.[7] Other compositions of $Sr_{1-x}M_xCuO_2$ with M = Ba,[8,9] Ca,[7-10] Pr,[11] Nd,[11-13] La,[13-15] Sm,[13] and Gd (Ref. 13) were stabilized in the IL structure using synthesis under high oxygen pressure and high temperature. Superconductivity was found in all of these compositions with $T_c \approx 80-110$ K for Ba, Ca, and $T_c \approx 40$ K for Nd, La, Sm, and Gd. The M = lanthanide samples are electron doped,

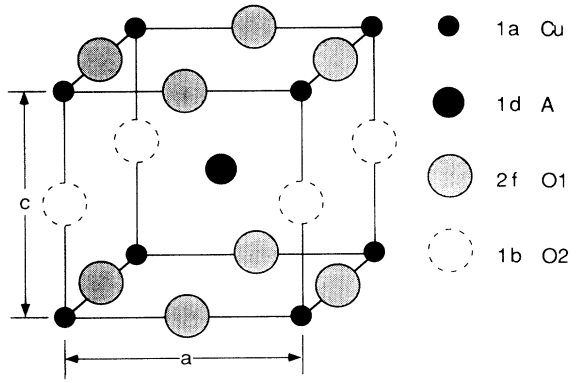

FIG. 1. The tetragonal crystal structure of the infinite layer $ACuO_2$ (A = alkaline metal, or a solid solution of alkaline with lanthanide metal) consists of alternately stacked A and CuO_2 layers. The Wyckoff site designation is given. The O2 site (dashed circles) is normally vacant in the infinite layer structure (it is fully occupied in the cubic perovskite structure).

are nearly phase pure and generally give large superconducting fractions.[12–15] The superconducting Ba and Ca samples are invariably phase impure, contain planar defects,[9,10,16] and give small superconducting fractions (SF < 20%).[9,10] It is speculated that in the M = Ba, Ca compounds, hole doping is caused by planar defects and/or A-site vacancies and/or oxygen nonstoichiometry.[9,10,16,17]

Studies of the pressure effect on T_c show that $dT_c/dP \approx 0.0$, 0.6, 0.7, and 2.1 K/GPa in $Sr_{0.92}Sm_{0.08}CuO_2$,[18] $Sr_{0.86}Nd_{0.14}CuO_2$,[12] $Sr_{0.7}Ca_{0.3}CuO_2$,[18] and $SrCuO_2$.[18] This result is consistent with what was found in many cuprate superconductors, namely, the pressure derivative of T_c for hole-doped compounds is generally larger than the derivative for electron-doped compounds.[1]

In the present paper we report the results of a neutron-diffraction study of the effect of pressure on the lattice constants of three compounds with the IL structure: an electron-doped superconductor, $Sr_{0.9}La_{0.1}CuO_2$ with $T_c = 42$ K and SF ≈ 70%;[15] a hole-doped superconductor, $Sr_{0.7}Ca_{0.3}CuO_2$ with $T_c = 99$ K and SF ≈ 4%; and a nonsuperconducting sample, $Sr_{0.14}Ca_{0.86}CuO_2$. The compressibilities obtained for these samples are compared with the results of first principles calculations[19] and with empirical predictions[20] for the IL structure. The $Sr_{0.7}Ca_{0.3}CuO_2$ sample contained orthorhombic[21] $Sr_4Cu_6O_{10}$ as a second phase, for which the compressibilities are also reported.

II. PREPARATION AND CHARACTERIZATION OF THE SAMPLES

The $Sr_{0.9}La_{0.1}CuO_2$ sample was prepared using high-pressure (5 GPa) and high-temperature (950 °C) synthesis. The details of the preparation were published previously.[15] The sample was a disk approximately 2 mm in diameter and 1 mm thick with a mass of 82 mg. Magnetic (ac) susceptibility measurements for this sample show[15] a well-defined superconducting transition at 42 K and a large diamagnetic signal (corresponding to a superconducting fraction of 70%) consistent with bulk superconductivity. The same sample was used in a previous neutron-diffraction study of the structure of $Sr_{0.9}La_{0.1}CuO_2$.[15]

The $Sr_{0.7}Ca_{0.3}CuO_2$ sample was obtained from starting materials which consisted of preformed low-pressure (orthorhombic) phases[22] of $(Sr_{0.7}Ca_{0.3})CuO_2$ and $(Sr_{0.7}Ca_{0.3})_2CuO_3$, which were mixed in molar ratio of 9:1. This ratio corresponds to a nominal composition of $(Sr_{0.7}Ca_{0.3})_{1.1}CuO_2$, which is inconsistent with the IL structure and will lead to the formation of a second phase (*vide infra*), unless defects are formed in large concentrations. The low-pressure phases were synthesized from high purity (99.995%) $SrCO_3$, $CaCO_3$, and CuO, which were mixed in agate mortar and pestle for 1 h, and prereacted at 950 °C for 15 h. The whole procedure was repeated five times. After phase-pure compounds were confirmed by x-ray diffraction, the appropriate proportions of the low-pressure phases were mixed and pressed at 800 Kg/cm^2. The pressed pellets (3 g), were loaded into a gold capsule, sandwiched between two pellets (0.3 g) of $KClO_4$. The thoroughly sealed capsule was loaded into an opposed anvil press and pressed at 5.7 GPa at 1050 °C for 1 h. An internal oxidizing atmosphere was produced in the capsule at high temperature by decomposition of $KClO_4$. At the end of 1 h, the sample was quenched to room temperature before releasing the pressure.

Small specimens taken from the sample were used for x-ray diffraction, electrical resistance, and magnetic susceptibility measurements. Specimens taken from the surface of the sample showed T_C is as high as 105 K and diamagnetic signals corresponding to superconducting fractions as high as 20%. The relatively large specimen of 0.56 g for neutron diffraction was taken from the core of the sample. Magnetic (ac) susceptibility measurements of a specimen from the neutron-diffraction sample show a well-defined superconducting transition at 99 K with a diamagnetic signal corresponding to a superconducting fraction of 4%. X-ray diffraction showed lines which do not belong to the IL structure and were identified as contributions from $Sr_4Cu_6O_{10}$ impurity.[21] Two-phase analysis of the neutron-diffraction data yielded (*vide infra*) a volume fraction of ≈ 15% for this phase. The nonsuperconducting phases of $Sr_{n-1}Cu_{n+1}O_{2n}$ form in an oxygen-deficient atmosphere,[17,21] whereas superconducting phases of $Sr_{n+1}Cu_nO_{2n+1}$ form in oxygen-rich atmosphere[22,23] during the high-pressure synthesis. These superconducting phases were found in small specimens taken from the surface of the sample and were not found in the specimen taken from the core of the sample for neutron diffraction. Formation of $Sr_4Cu_6O_{10}$ therefore suggests oxygen deficiency at the core of the sample during the high-pressure synthesis.

The $Sr_{0.14}Ca_{0.86}CuO_2$ sample was synthesized by intimately mixing $SrCO_3$, $CaCO_3$, and CuO (all 999.99%) in the proportions 0.14:0.86:1. The mixture was fired in air

TABLE I. Description of the three samples and the method used for mounting them in the pressure cell. The number of pressure steps (including ambient pressure) and total run time are also given.

Sample	Mass g	Form	Mounting	Number of pressure steps	Total run time (h)
$Sr_{0.9}La_{0.1}CuO_2$	0.082	Solid piece	Suspended	5	35
$Sr_{0.7}Ca_{0.3}CuO_2$	0.56	Solid piece	Suspended	6	55
$Sr_{0.14}Ca_{0.86}CuO_2$	≈ 10	Powder	Vanadium can	7	4

at 920–950° C for 48 h with frequent intermediate grindings. Final firing was done for one week at 950 °C, followed by fast cooling to room temperature. X-ray diffraction showed that the resulting material is phase pure with the IL structure.

III. HIGH-PRESSURE NEUTRON-DIFFRACTION MEASUREMENTS AND ANALYSIS

A He-gas pressure cell (described previously[24]) was used to control the pressure on the sample in the neutron beam. In order to minimize neutron background, the two small samples ($Sr_{0.9}La_{0.1}CuO_2$ and $Sr_{0.7}Ca_{0.3}CuO_2$, Table I) were supported in the neutron beam inside the pressure cell by a boron-coated tungsten fiber. The He-gas pressure cell offers the advantage of hydrostatic conditions, precise pressure measurements, and (owing to the fixed-angle time-of-flight technique) diffraction data that are completely free from Bragg scattering from the cell. For each sample, neutron-diffraction data were taken at room temperature at several pressures (including ambient pressure, Table I) on the Special Environment Powder Diffractometer at the Intense Pulsed Neutron Source (IPNS).[25] The data were taken at the two 90 deg detector banks. Total data collecting times were about 35, 55, and 4 h for the $Sr_{0.9}La_{0.1}CuO_2$, $Sr_{0.7}Ca_{0.3}CuO_2$, $Sr_{0.14}Ca_{0.86}CuO_2$ samples, respectively.

The IPNS program for Rietveld analysis of the time-of-flight neutron-diffraction data[26] was used to analyze the pattern taken at each pressure. In this analysis the structural parameters of the sample are refined so that the calculated pattern will best fit (least squares) the observed pattern. The analyses were performed using the

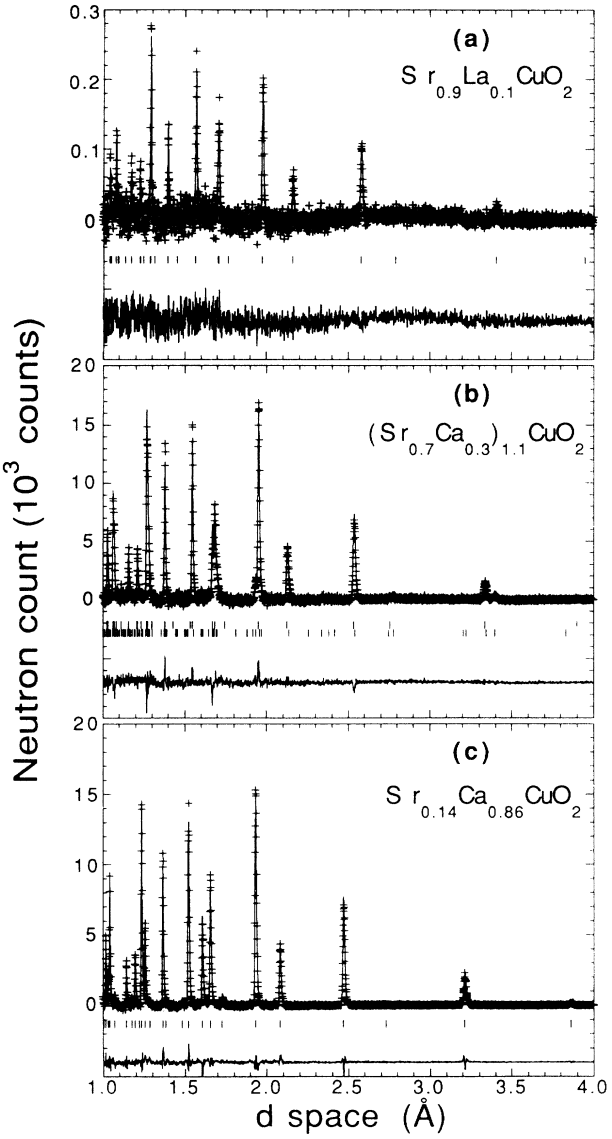

FIG. 2. Portion of a typical Rietveld refinement profile for: (a) $Sr_{0.9}La_{0.1}CuO_2$ at 0.16 (GPa); (b) $Sr_{0.7}Ca_{0.3}CuO_2$ at 0.59 (GPa); (c) $Sr_{0.14}Ca_{0.86}CuO_2$ at 0.1 (GPa). The plus signs (+) represent the raw time-of-flight neutron-powder-diffraction data. The solid line represents the calculated profile. Tick marks represent the positions of the allowed Bragg reflections. The second phase in the $Sr_{0.7}Ca_{0.3}CuO_2$ sample is $Sr_4Cu_6O_{10}$. The background was fit as part of the refinement, but has been subtracted prior to plotting. A difference curve (observed-calculated) is plotted at the bottom.

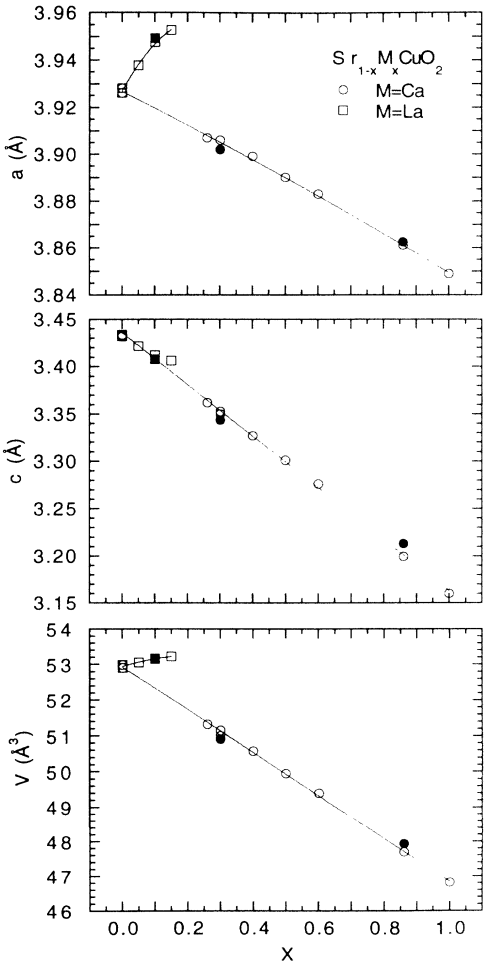

FIG. 3. The dependence of the lattice constants a and c on the content of M in $Sr_{1-x}M_xCuO_2$ [M=Ca (Refs. 6, 8, 10, 29, and 30), La (Ref. 14)]. Results from the literature are represented by open symbols. The lattice constants of the three samples of the present work are represented by closed symbols. The unit-cell volume, V, is calculated from the lattice constants.

space group $P4/mmm$ (Ref. 27) for the infinite layer structure. A two-phase analysis was used for the $Sr_{0.7}Ca_{0.3}CuO_2$ sample, which contained $Sr_4Cu_6O_{10}$ as a second phase. Using the space group *Cmmm* (Refs. 21 and 27) for the second phase, the analysis yielded a volume fraction of about 15% of $Sr_4Cu_6O_{10}$ in this sample. The thermal factors of all the atoms and the linewidth were allowed to vary in the analysis and were found to be independent (within the experimental uncertainty) of pressure. A summary of the results for the three samples at ambient pressure is given in Table II. Observed and calculated profiles for the three samples are shown in Fig. 2.

IV. RESULTS AND DISCUSSION

The ambient pressure lattice constants as determined in the present work (Table II) for the three samples are in good agreement with values from the literature[6,8,10,14,29,30] (Fig. 3). This agreement corroborates the nominal composition of the samples. The pressure-induced changes in the lattice constants and in the unit-cell volume are shown in Figs. 4–7 for $Sr_{0.9}La_{0.1}CuO_2$, $Sr_{0.7}Ca_{0.3}CuO_2$, $Sr_{0.14}Ca_{0.86}CuO_2$, and $Sr_4Cu_6O_{10}$, respectively. The observed compressibilities which were obtained from linear fits to these changes are given in Table III. The compressibilities of the four cuprates are similar and have large compressibility anisotropy. The structure of $Sr_4Cu_6O_{10}$ is similar to the IL structure, which may explain the similarity in the compressibilities [it consists of Cu-deficient CuO_2 layers (containing CuO double chains) separated by a layer of Sr (Ref. 21)].

The large compressibility anisotropy ($\kappa_a/\kappa_c \approx 0.5$) observed in the present work is in a good agreement with the prediction ($\kappa_a/\kappa_c \approx 0.48$) of a recent calculation of the compressibilities in the IL structure using first-principles total energy calculations.[19] These calculations which are based on the lattice parameters reported[10] for $Sr_{0.7}Ca_{0.3}CuO_2$ predict $\kappa_a, \kappa_c, \kappa_V \approx 2\times10^{-3}$, 4.23×10^{-3}, 8.22×10^{-3} (GPa^{-1}), in excellent agreement with the measured values of $2.2(1)\times10^{-3}$, $4.07(9)\times10^{-3}$, $8.5(3)\times10^{-3}$ (GPa^{-1}) for $Sr_{0.7}Ca_{0.3}CuO_2$ (Table III).

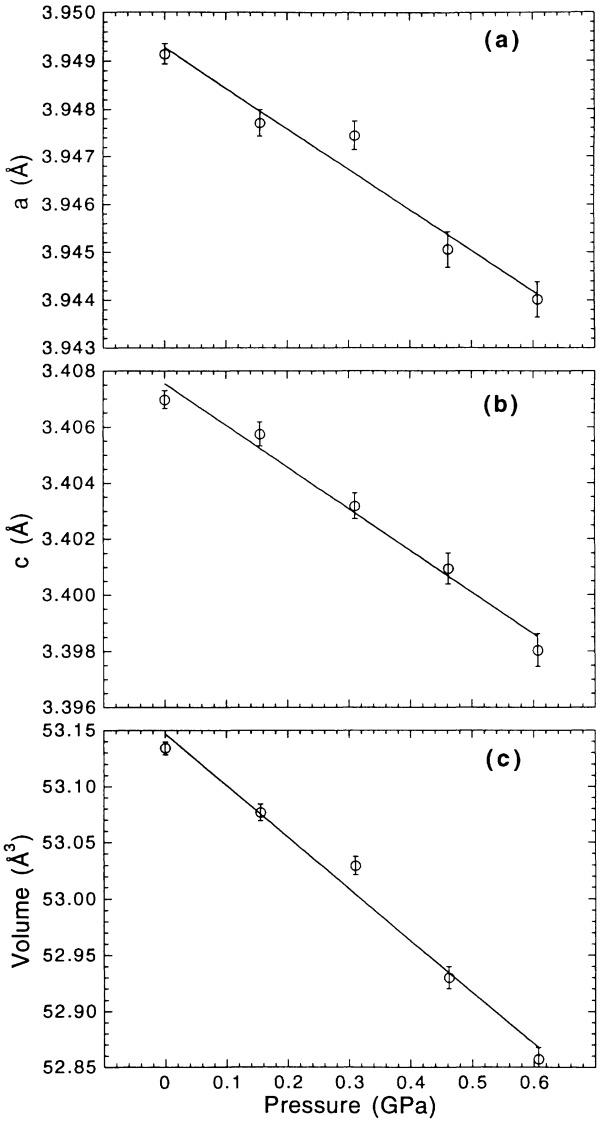

FIG. 4. The measured lattice constant, a (a); lattice constant, c (b), and unit-cell volume, V (c) as a function pressure, for $Sr_{0.9}La_{0.1}CuO_2$. The error bars represent statistical standard deviations taken from the Rietveld refinements.

TABLE II. Refined structural parameters for the four phases at ambient pressure. Rietveld refinements were done in the tetragonal $P4/mmm$ space group (Ref. 27) for the IL phases (columns 2–4) and in the orthorhombic *Cmmm* space group (Ref. 27) for $Sr_4Cu_6O_{10}$. Atom positions in $P4/mmm$ are A at 1*d* (1/2,1/2,1/2), Cu at 1a (0,0,0), O1 at 2*f* (1/2,0,0). Scattering amplitudes (in units of 10^{-12} cm) (Ref. 28): 0.702, 0.827, 0.49, 0.7719, and 0.5803 were used for Sr, La, Ca, Cu, and O, respectively. The occupancy of the A site was fixed at the nominal composition for each sample. Numbers in parentheses are statistical errors of the last significant digit.

Sample	$Sr_{0.9}La_{0.1}CuO_2$	$Sr_{0.7}Ca_{0.3}CuO_2$	$Sr_{0.14}Ca_{0.86}CuO_2$	$Sr_4Cu_6O_{10}$
a (Å)	3.9491(2)	3.9032(1)	3.8635(1)	3.9145(9)
b (Å)				19.354(3)
c (Å)	3.4070(3)	3.3449(1)	3.2131(1)	3.4061(5)
V (Å^3)	53.134(6)	50.959(3)	47.937(2)	258.07(7)
$B(A)$ (Å^2)	0.2(1)	0.46(6)	0.60(3)	
B(Cu) (Å^2)	0.5(1)	0.31(5)	0.28(2)	
B(O1) (Å^2)	0.3(1)	0.58(4)	0.64(3)	
R_{WP} (%)	19.0	10.9	14.5	10.9
R_{exp} (%)	16.2	9.2	12.8	9.2

TABLE III. Linear compressibilities, compressibility anisotropies, volume compressibilities, and bulk moduli. Numbers in parentheses represent standard deviations of the last significant digit.

Sample	$Sr_{0.9}La_{0.1}CuO_2$ 1	$Sr_{0.7}Ca_{0.3}CuO_2$ 2	$Sr_{0.14}Ca_{0.86}CuO_2$ 3	$Sr_4Cu_6O_{10}$ 2
κ_a (10^{-3} GPa^{-1})	2.2(3)	2.2(1)	1.89(3)	2.4(3)
κ_b (10^{-3} GPa^{-1})				2.2(2)
κ_c (10^{-3} GPa^{-1})	4.2(3)	4.07(9)	4.68(5)	5.3(4)
κ_a/κ_c	0.53(8)	0.55(3)	0.403(8)	0.47(7)
κ_b/κ_c				0.41(5)
κ_b/κ_a				0.9(1)
κ (10^{-3} GPa^{-1})	8.6(7)	8.5(3)	8.44(6)	9.9(4)
B (GPa)	117(10)	118(4)	118.5(9)	102(5)

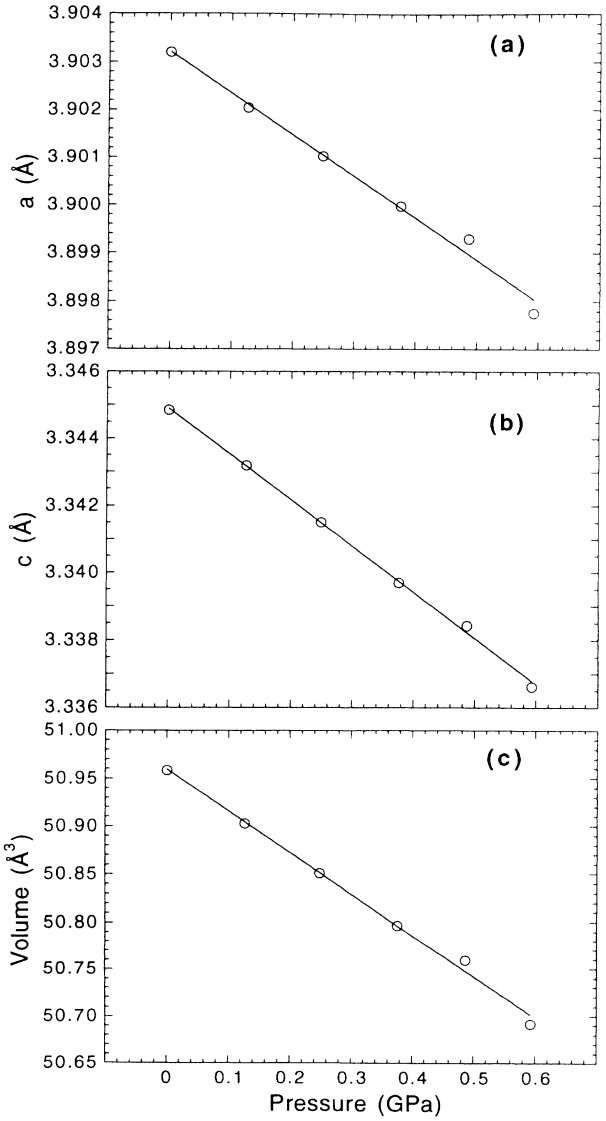

FIG. 5. The measured lattice constant, a (a); lattice constant, c (b) and unit-cell volume, V (c) as a function pressure, for $Sr_{0.7}Ca_{0.3}CuO_2$. The statistical standard deviations taken from the Rietveld refinements are smaller than the symbols and are not shown.

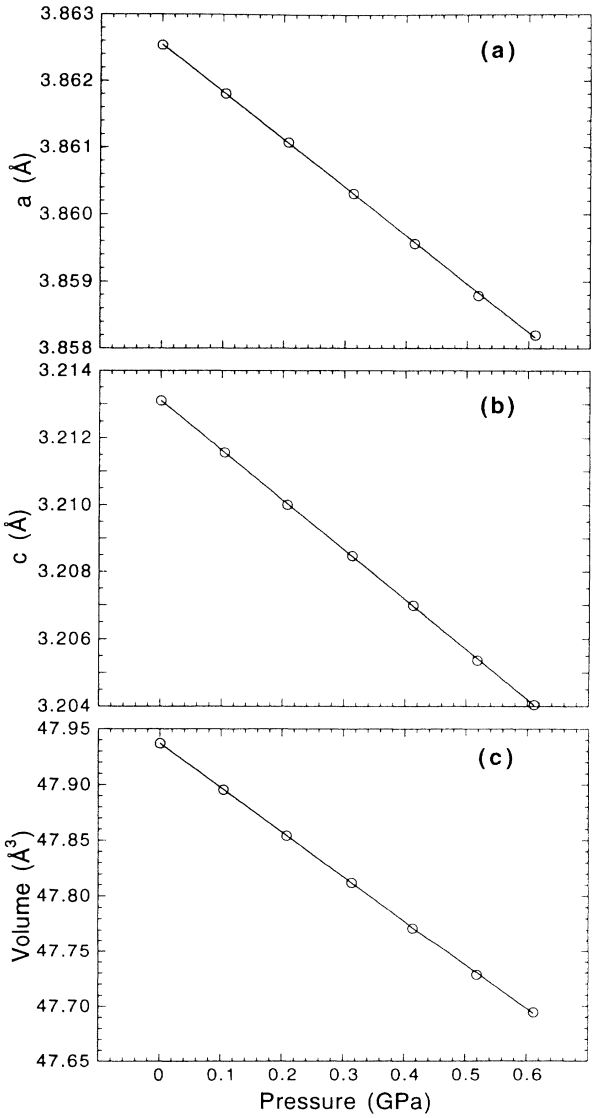

FIG. 6. The measured lattice constant, a (a); lattice constant, c (b) and unit-cell volume, V (c) as a function pressure, for $Sr_{0.14}Ca_{0.86}CuO_2$. The statistical standard deviations taken from the Rietveld refinements are smaller than the symbols and are not shown.

This agreement with the calculations (in which crystal lattices are refined to give minimum electronic energies) suggests that the compressibilities are largely determined by the electronic structure.

The measured compressibilities of $Sr_{0.9}La_{0.1}CuO_2$, $Sr_{0.7}Ca_{0.3}CuO_2$, and $Sr_{0.14}Ca_{0.86}CuO_2$ are compared in Table IV to the results of empirical calculations which use the concept of comparative crystal chemistry.[20] There is general qualitative agreement, however, the calculated κ_c and κ values are systematically higher than the measured values. We have no explanation for this systematic discrepancy. It is interesting to point out that $Sr_{0.9}La_{0.1}CuO_2$ (electron doped) and $Sr_{0.7}Ca_{0.3}CuO_2$ (hole doped) have the same compressibilities. This is consistent with recent measurements[31] of the compressibilities of $Nd_{1.835}Ce_{0.165}CuO_4$ (electron doped) which are found to be essentially the same as hole-doped superconductors with the same structure.[1]

The increase of T_c with pressure in $Sr_{0.7}Ca_{0.3}CuO_2$ and $SrCuO_2$ (Ref. 18) suggests that T_c can be increased at ambient pressure if the system is suitably modified.[1] Figure 3 shows how the lattice parameters are modified by changing the size (M=Ca) and the size and charge (M=La) of the A atom in $ACuO_2$. It is interesting to compare the pressure effect with this size effect on the crystal lattice. The response of the lattice parameters to changing the size and charge of the A atom in $ACuO_2$ is illustrated in Fig. 8. As Sr^{2+} ($r_{eff} \approx 1.26$ Å) is replaced by the smaller Ca^{2+} the two lattice parameters decrease linearly with r_{eff}, suggesting a pure size effect. When Sr^{2+} is replaced by the smaller La^{3+} or Nd^{3+} ions, electron doping of the Cu-O bond causes it to expand resulting in an increase in a. The variation of c with r_{eff} fits a single straight line for Ca^{2+}, La^{3+}, and Nd^{3+} and is in-

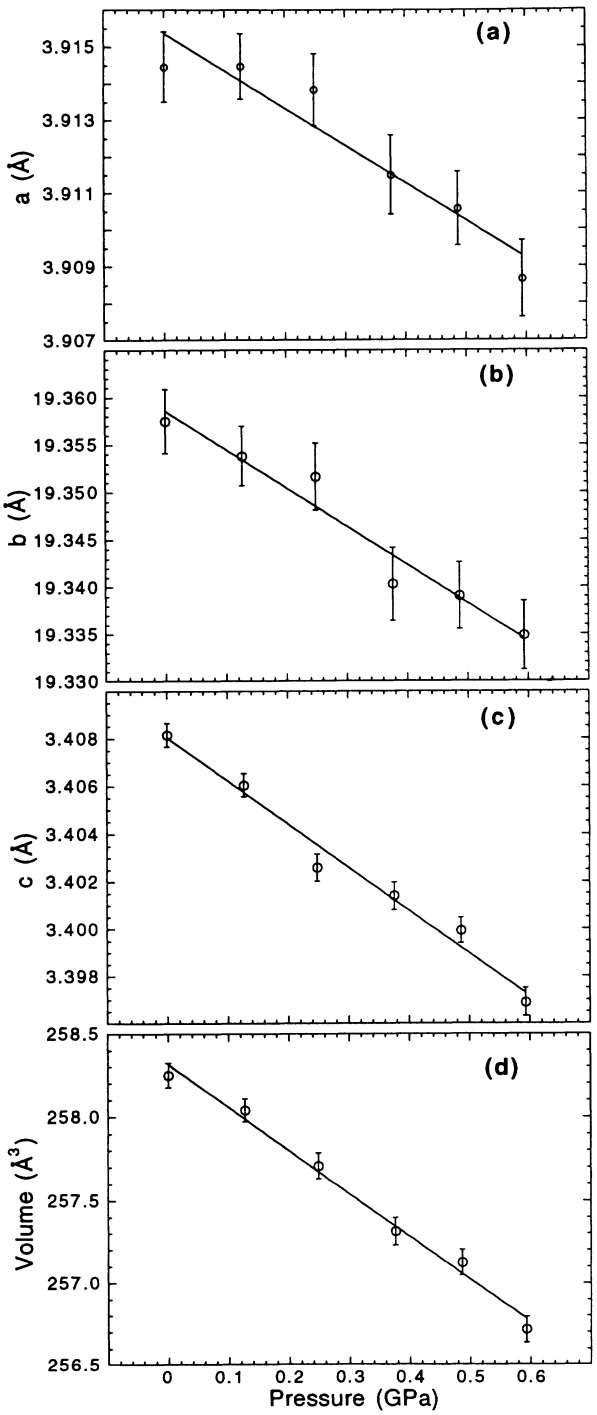

FIG. 7. The measured lattice constant, a (a); lattice constant, b (b); lattice constant, c (c), and unit-cell volume, V (d) as a function pressure, for $Sr_4Cu_6O_{10}$ (second phase in the $Sr_{0.7}Ca_{0.3}CuO_2$ sample). The error bars represent statistical standard deviations taken from the Rietveld refinements.

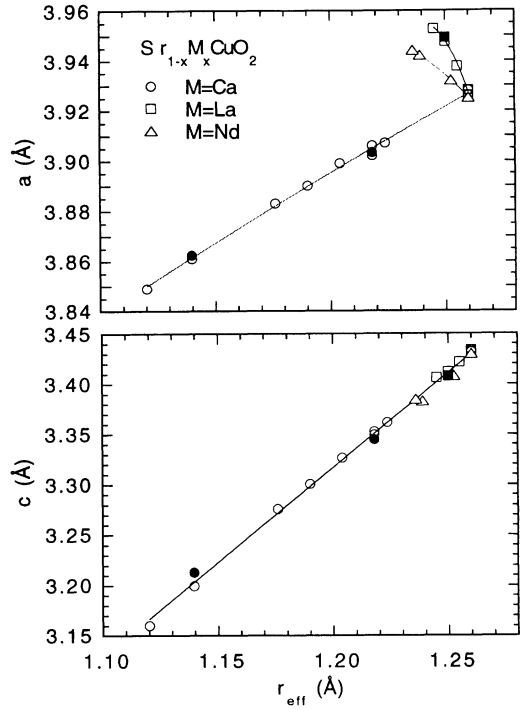

FIG. 8. Lattice parameters in $Sr_{1-x}M_xCuO_2$ [M=Ca (Refs. 6, 8, 10, 29, and 30), La (Ref. 14), Nd (Ref. 11)] vs the effective radius, r_{eff}, where $r_{eff}=(1-x)r_{Sr}+xr_M$. The following ionic radii with eightfold coordination were used (Ref. 32): $r_{Sr}=1.26$, $r_{Ca}=1.12$, $r_{La}=1.160$, and $r_{Nd}=1.109$ (Å). Results from the literature are represented by open symbols. Closed symbols represent results of the present work.

TABLE IV. Measured (present work) and predicted [results of empirical calculations (Ref. 20)] values of linear compressibilities. Numbers in parentheses represent standard deviations of the last significant digit.

	$Sr_{0.9}La_{0.1}CuO_2$		$Sr_{0.7}Ca_{0.3}CuO_2$		$Sr_{0.14}Ca_{0.86}CuO_2$	
	Meas.	Calc.	Meas.	Calc.	Meas.	Calc.
$\kappa_a(10^{-3}$ GPa$^{-1})$	2.2(3)	2.4	2.2(1)	2.2	1.89(3)	2.2
$\kappa_c(10^{-3}$ GPa$^{-1})$	4.2(3)	5.9	4.07(9)	5.5	4.68(5)	5.3
κ $(10^{-3}$ GPa$^{-1})$	8.6(7)	10.7	8.5(3)	9.9	8.44(6)	9.7

dependent of doping, consistent with a pure size effect. The response of a and c to the size of A can be characterized by the respective derivatives: da/dr_{eff} and dc/dr_{eff} which equal 0.528 and 1.896, respectively. This can be compared with the respective pressure derivatives da/dp and dc/dp which are equal to 0.008 59 and 0.013 61 (Å/GPa), respectively. This result shows that the size anisotropy (i.e., dc/da) is equal to 3.6, compared to a pressure anisotropy of 1.6.

The a vs r_{eff} line represents data of essentially undoped nonsuperconducting samples.[8] The a value for the superconducting (SF$\approx$4%) $Sr_{0.7}Ca_{0.3}CuO_2$ sample of the present work (closed circle at $r_{\text{eff}}\approx 1.22$ Å in Fig. 8) concurs with this line, hence, showing no doping of the Cu-O bond (within the experimental accuracy). There are three possible explanations to this result: (i) If only 4% ($\approx$SF) of the IL structure is doped, the bulk of the sample (i.e., 96%) does not show a lattice change, and the lattice change of the small (i.e., 4%) portion of the sample is not detected by the present neutron-diffraction analysis. (ii) The phase with the IL structure is not the superconducting phase, or (iii) as previously suggested,[10,16] superconductivity is associated with planar defects. None of these possibilities can be ruled out using the data of the present work.

In the IL structure, the compressibility κ_a is essentially the compressibility of the CuO_2 layer. In other HTSC's, there are other layers which affect the in-plane compressibility. However, the CuO_2 layer is the most densely packed among these layers and is therefore expected to be the major contributor to the in-plane compressibility, κ_a. Hence, the in-plane compressibility will decrease as the linear density of these planes, n/c (i.e., number of planes per unit length along c), increases. Consider, for example, the series of structures Hg-1 2 $n-1$ n ($n=1,2,3,\ldots$);[5] The linear density, n/c, increases monotonically with n, reaching a maximum value at $n=\infty$ (i.e., for the infinite layer structure). The in-plane compressibility, κ_a, is therefore expected to decrease monotonically with n and reach a minimum value at $n=\infty$. This behavior is clearly delineated in Fig. 9, consistent with the hypothesis that the major contribution to κ_a comes from the CuO_2 layers.

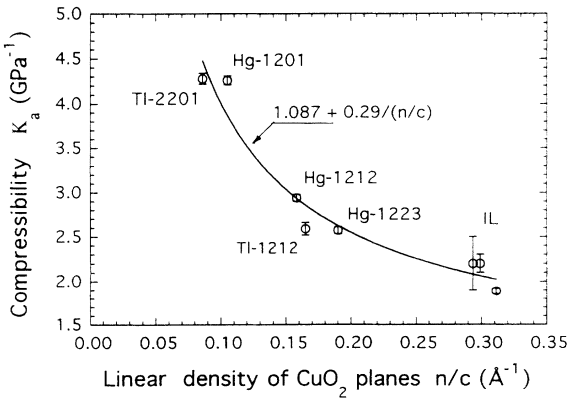

FIG. 9. The relation between the in-plane compressibility, κ_a, measured in some $n=1,2,3$ (Refs. 5, 31, and 33) and ∞ (present work) layer HTSC's, and the linear density of CuO_2 layers. The infinite layer results are given (from left to right) for $Sr_{0.9}La_{0.1}CuO_2$, $Sr_{0.7}Ca_{0.3}CuO_2$, and $Sr_{0.14}Ca_{0.86}CuO_2$. The solid line represents the best fit (least squares) to the data.

V. CONCLUSIONS

The compressibilities of three compositions in the IL structure $Sr_{0.9}La_{0.1}CuO_2$, $Sr_{0.7}Ca_{0.3}CuO_2$, $Sr_{0.14}Ca_{0.86}CuO_2$, superconducting electron doped, hole doped, and nonsuperconducting were measured and were found to be highly anisotropic and essentially independent of composition. The measured values are in a good agreement with first-principles calculation performed for undoped $Sr_{0.7}Ca_{0.3}CuO_2$. The response of the crystal lattice to an increase of the atomic size of A in $ACuO_2$, is highly anisotropic, with the c axis 3.6 times softer than the a axis. The compressibility of the CuO_2 lattice governs the in-plane compressibility in n-layered ($n=1,2,3\ldots,\infty$) cuprates. Consequently, κ_a increases as the inverse of the linear density of the CuO_2 planes, n/c.

ACKNOWLEDGMENTS

We would like to acknowledge useful discussions with A. J. Freeman. This work was supported by U.S. Department of Energy, Division of Basic Energy Sciences–Material Science, under Contract No. W-31-109-ENG-38 (J.D.J., R.L.H., B.D.), the National Science Foundation, Science and Technology Center for Superconductivity under Grant No. DMR 91-20000 (H.S., B.A.H., P.G.R.), the Nuclear Research Center–Negev and Ben-Gurion University in the Negev, (H.S.), and the NEC Corporation, Japan (Y.S.). The Intense Pulsed Neutron Source is operated as a user facility by the U. S. Department of Energy, Division of Basic Energy Sciences–Material Science, under Contract No. W-31-109-ENG-38.

*Permanent address: Department of Physics, Nuclear Research Center–Negev, P.O.B. 9001, Beer-Sheva, Israel 84190 and Department of Physics, Ben-Gurion University of the Negev, P.O.B. 653, Beer-Sheva, Israel 84105.

†Permanent address: Fundamental Research Laboratories, NEC Corporation, 34 Miyukigaoka, Tsukuba 305, Japan.

[1]J. S. Schilling and S. Klotz, in *Physical Properties of High Temperature Superconductors III,* edited by D. M. Ginsberg (World Scientific, Singapore, 1992), p. 59.

[2]A. K. Klehe, J. S. Schilling, J. L. Wagner, and D. G. Hinks, Physica C **223**, 313 (1994).

[3]C. W. Chu, L. Gao, F. Chen, Z. J. Huang, R. L. Meng, and Y. Y. Xue, Nature **365**, 323 (1993).

[4]L. Gao, Y. Y. Xue, F. Chen, Q. Xiong, R. L. Meng, D. Ramirez, C. W. Chu, J. H. Eggert, and H. K. Mao, Phys. Rev. B **50**, 4260 (1994).

[5]B. A. Hunter, J. D. Jorgensen, J. L. Wagner, P. G. Radaelli, D. G. Hinks, H. Shaked, R. L. Hitterman, and R. B. Von Dreele, Physica C **221**, 1 (1994).

[6]T. Siegrist, S. M. Zahurak, D. W. Murphy, and R. S. Roth, Nature **334**, 231 (1988).

[7]R. S. Roth, C. J. Rawn, J. J. Ritter, and B. P. Borton, J. Am. Ceram. Soc. **72**, 1545 (1989).

[8]M. Takano, Y. Takeda, H. Okada, M. Miyamoto, and T. Kusaka, Physica C **159**, 375 (1989).

[9]M. Takano, M. Azuma, Z. Hiroi, Y. Bando, and Y. Takeda, Physica C **176**, 441 (1991).

[10]M. Azuma, Z. Hiroi, M. Takano, Y. Bando, and Y. Takeda, Nature **356**, 775 (1992).

[11]M. G. Smith, A. Manthiram, J. Zhou, J. B. Goodenough, and J. T. Markert, Nature **351**, 549 (1991).

[12]C. L. Wooten, Beom-hoan O, J. T. Markert, M. G. Smith, A. Manthiram, J. Zhou, and J. B. Goodenough, Physica C **192**, 13 (1992).

[13]N. Ikeda, Z. Hiroi, M. Azuma, M. Takano, Y. Bando, and Y. Takeda, Physica C **210**, 367 (1993).

[14]G. Er, Y. Miyamoto, F. Kanamaru, and S. Kikkawa, Physica C **181**, 206 (1991).

[15]J. D. Jorgensen, P. G. Radaelli, D. G. Hinks, J. L. Wagner, S. Kikkawa, G. Er, and F. Kanamaru, Phys. Rev. B **47**, 14 654 (1993).

[16]H. Zhang, Y. Y. Wang, V. P. Dravid, L. D. Marks, P. Han, D. A. Payne, P. G. Radaelli, and J. D. Jorgensen, Nature **370**, 352 (1994).

[17]M. Takano, J. Supercond. **7**, 49 (1994).

[18]H. Takahashi, N. Mori, M. Azuma, Z. Hiroi, and M. Takano, Physica C **227**, 395 (1994).

[19]D. L. Novikov, O. N. Mryasov, and A. J. Freeman, Physica C **219**, 246 (1994).

[20]A. L. Cornelius, S. Klotz, and J. S. Schilling, Physica C **197**, 209 (1992).

[21]Z. Hiroi, M. Azuma, M. Takano, and Y. Bando, J. Solid State Chem. **95**, 230 (1991).

[22]C. L. Teske and H. Muller-Buschbaum, Z. Anorg. Allgem. Chem. **379**, 234 (1970).

[23]Z. Hiroi, M. Takano, M. Azuma, and Y. Takeda, Nature **364**, 315 (1993).

[24]J. D. Jorgensen, S. Pei, P. Lightfoot, D. G. Hinks, B. W. Veal, B. Dabrowski, A. P. Paulikas, R. Kleb, and I. D. Brown, Physica C **171**, 93 (1990).

[25]J. D. Jorgensen, J. Faber, Jr., J. M. Carpenter, R. K. Crawford, J. R. Haumann, R. L. Hitterman, R. Kleb, G. E. Ostrowski, F. J. Rotella, and T. G. Worlton, J. Appl. Crystallogr. **22**, 321 (1989).

[26]F. J. Rotella (unpublished); R. B. Von Dreele, J. D. Jorgensen, and C. G. Windsor, J. Appl. Crystallogr. **15**, 581 (1982).

[27]*International Tables for Crystallography, Volume A, Space-Group Symmetry,* edited by T. Hahn (Reidel, Dordrecht, 1987), p. 468.

[28]*International Tables for Crystahlography, Volume C, Mathematical, Physical and Chemical Tables,* edited by A. J. C. Wilson (Reidel, Dordrecht, 1983), p. 384.

[29]Z. Hiroi, M. Azuma, M. Takano, and Y. Takeda, Physica C **208**, 286 (1993).

[30]G. Berghöfer, W. Pietzuch, and D. Reinen, J. Solid State Chem. **108**, 395 (1994).

[31]T. Kamiyama, F. Izumi, H. Takahashi, J. D. Jorgensen, B. Dabrowski, R. L. Hitterman, D. G. Hinks, H. Shaked, T. O. Mason, and M. Seabaugh, Physica C **229**, 377 (1994).

[32]R. D. Shannon, Acta Cryst. A **32**, 751 (1976).

[33]F. Izumi, J. D. Jorgensen, Y. Shimakawa, Y. Kubo, T. Manako, Shiyou Pei, T. Matsumoto, R. L. Hitterman, and Y. Kanke, Physica C **193**, 426 (1992).

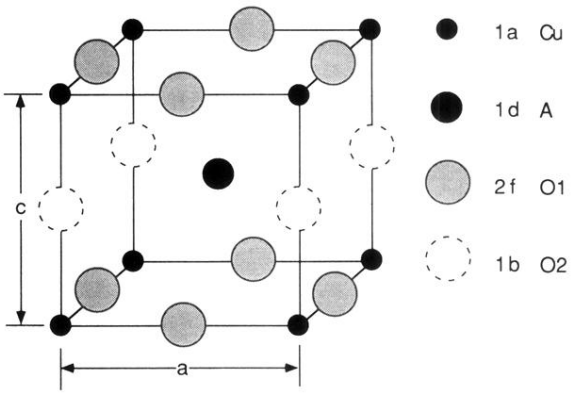

FIG. 1. The tetragonal crystal structure of the infinite layer $ACuO_2$ (A =alkaline metal, or a solid solution of alkaline with lanthanide metal) consists of alternately stacked A and CuO_2 layers. The Wyckoff site designation is given. The O2 site (dashed circles) is normally vacant in the infinite layer structure (it is fully occupied in the cubic perovskite structure).